

Experimental study of the effect of quantum-well structures on the thermoelectric figure of merit

L. D. Hicks

Department of Physics, Massachusetts Institute of Technology, Cambridge, Massachusetts 02139

T. C. Harman

Lincoln Laboratory, Massachusetts Institute of Technology, Lexington, Massachusetts 02173-9108

X. Sun

Department of Physics, Massachusetts Institute of Technology, Cambridge, Massachusetts 02139

M. S. Dresselhaus

Department of Electrical Engineering and Computer Science and Department of Physics, Massachusetts Institute of Technology, Cambridge, Massachusetts 02139

(Received 11 January 1996)

Recently, it has been shown theoretically that it may be possible to increase the thermoelectric figure of merit (Z) of certain materials by preparing them in the form of two-dimensional quantum-well structures. Using $\text{PbTe}/\text{Pb}_{1-x}\text{Eu}_x\text{Te}$ multiple-quantum-well structures grown by molecular-beam epitaxy, we have performed thermoelectric and other transport measurements as a function of quantum-well thickness and doping. Our results are found to be consistent with theoretical predictions and indicate that an increase in Z over bulk values may be possible through quantum confinement effects using quantum-well structures.

For a good thermoelectric material for cooling applications, the material must have a high thermoelectric figure of merit, Z . The figure of merit is defined by¹

$$Z = \frac{S^2 \sigma}{\kappa} \quad (1)$$

where S is the thermoelectric power (Seebeck coefficient), σ is the electrical conductivity, and κ is the thermal conductivity. In order to achieve a high Z , one requires a high thermoelectric power S , a high electrical conductivity σ , and a low thermal conductivity κ . In general, it is difficult to increase Z for the following reasons: Increasing S for simple materials also leads to a simultaneous decrease in σ , and an increase in σ leads to a comparable increase in the electronic contribution to κ because of the Wiedemann-Franz law. So with known conventional solids, a limit is rapidly obtained where a modification to any one of the three parameters S , σ , or κ , adversely affects the other transport coefficients, so that the resulting Z does not vary significantly. Currently, the materials with the highest Z are Bi_2Te_3 alloys such as $\text{Bi}_{0.5}\text{Sb}_{1.5}\text{Te}_3$, with $ZT \approx 1.0$ at $T = 300$ K.¹ Only small increases in Z have been achieved in the last two decades, so it is now felt that the Bi_2Te_3 compounds may be nearing the limit of their potential performance.

In earlier papers,^{2,3} we considered theoretically the effect on Z of using materials in two-dimensional (2D) structures such as 2D multiple-quantum-well (MQW) structures, and showed that this approach could yield a significant increase in Z over the bulk value as the quantum-well width is decreased. The proposed increase in Z arises mainly from the enhancement of the density of electron states per unit volume that occurs for small well widths. Other workers have extended our initial calculation and have confirmed that an in-

crease in Z over bulk values may be possible for narrow well widths.⁴⁻⁶ In this paper, we report an experimental investigation to test our theoretical predictions.

The MQW system used for the investigation is the $\text{PbTe}/\text{Pb}_{1-x}\text{Eu}_x\text{Te}$ system. This system was chosen for our thermoelectric investigation for the following reasons. Firstly, the fabrication technology is relatively well developed, making it possible to grow samples with high mobility 2D transport and to have precise control over the carrier density. Secondly, bulk PbTe is a relatively good thermoelectric material with a ZT of 0.4 at 300 K, so that a reasonable increase in Z due to 2D effects could perhaps result in a Z higher than the best Bi_2Te_3 alloys. In the $\text{PbTe}/\text{Pb}_{1-x}\text{Eu}_x\text{Te}$ system, the PbTe is the quantum well and $\text{Pb}_{1-x}\text{Eu}_x\text{Te}$ is the barrier material. Such structures have a type-I band alignment and a nearly symmetric offset between valence and conduction bands.⁷ The energy gap of the $\text{Pb}_{1-x}\text{Eu}_x\text{Te}$ barrier increases strongly with x , the Eu content,⁸ so only about 6% Eu can give large confinement energies and yield 2D transport for electrons in the PbTe quantum wells.⁹ The mobility of $\text{Pb}_{1-x}\text{Eu}_x\text{Te}$ also decreases rapidly with increasing Eu content.⁹

Our proposed increase in Z in MQW structures occurs in the quantum wells alone. In order to extract easily the well transport properties from our MQW results, we needed to grow samples for which transport is dominated by 2D conduction in the wells, with negligible barrier conduction. Using mobility measurements,¹⁰ we found that samples dominated by well conduction could be obtained at 300 K using a barrier Eu content of $x > 0.07$ and barrier widths larger than 350 Å. We measured MQW mobilities of over 1400 $\text{cm}^2 \text{V}^{-1} \text{s}^{-1}$, which is comparable to our best PbTe single layer samples of 1600 $\text{cm}^2 \text{V}^{-1} \text{s}^{-1}$. Since the mobility of our barrier layers (45 $\text{cm}^2 \text{V}^{-1} \text{s}^{-1}$) is much lower than the

wells, the mobility of a MQW sample should be significantly less than bulk PbTe if there were significant conduction in the barrier region.

According to our model,² the increase in Z due to 2D effects arises mainly from the power factor $S^2\sigma$, while the lattice thermal conductivity is assumed to be unchanged from the bulk value except for well widths less than about 10 Å. In fact, we also assumed that the mobility of the quantum well would be the same as the best bulk value—an assumption that we verified experimentally—so any increase in Z would arise through the factor S^2n , where n is the carrier density in the quantum well. Therefore, according to our model, we should be able to observe an increase in S^2n as the well width is narrowed.

Samples were grown by molecular-beam epitaxy (MBE) in a modified Varian 360 MBE system. Details of the sample preparation and characterization are given elsewhere.¹⁰ Briefly, first a $\text{Pb}_{0.958}\text{Eu}_{0.042}\text{Te}$ buffer of about 2000 Å was deposited on a freshly cleaved $\text{BaF}_2(111)$ substrate. Next, superlattice samples with 100 to 150 periods of $\text{PbTe}/\text{Pb}_{0.927}\text{Eu}_{0.073}\text{Te}$ MQW structures were grown, with PbTe well widths varying between 17 and 55 Å, separated by wide $\text{Pb}_{0.927}\text{Eu}_{0.073}\text{Te}$ barriers of about 450 Å. The carrier density was varied by using Bi donor atoms in the barrier material. This resulted in an n -type material so that all the electrical conduction is in the conduction-band quantum well.

The resistivity, Hall coefficient, and Seebeck coefficient of the samples were measured at 300 K. Contacts were made with an In alloy, which results in excellent ohmic contacts for n -type samples. Chromel-Alumel thermocouples were used in measuring the Seebeck coefficient. Since we had already established that virtually all the conduction in our MQW samples is in the PbTe well and that barrier electronic conduction can be neglected, we were able to focus our attention on the transport properties of the quantum well alone. Thus the carrier density in the quantum wells could be calculated directly from the Hall coefficient and the well width. Also, the Seebeck coefficient of the wells was equal to the measured S of the MQW sample. For each sample, the value of the well S^2n was obtained and the results are shown in Fig. 1 as full circles. Figure 1(a) shows the results as a function of well thickness a , and Fig. 1(b) shows S^2n as a function of carrier density n . The corresponding results for bulk single-crystal PbTe obtained from Ref. 10 are also shown on these plots. The data points in Fig. 1(a) show an increase in S^2n as the well width is narrowed, and the well S^2n may reach several times the bulk value for small well widths. This result is predicted by our theoretical model and therefore gives qualitative support to the idea that MQW structures may be used to improve Z over bulk values. To obtain a quantitative comparison between experiment and theory, we used our model to calculate values of S^2n vs a and vs n for the $\text{Pb}_{0.927}\text{Eu}_{0.073}\text{Te}$ MQW system as described below.

In our original model,² we considered a quantum well in which only a single subband contributes to the transport and to Z . However, in a PbTe quantum well there are two sets of subbands that may contribute to the transport, arising from the four degenerate valleys at the L points of the Brillouin zone in bulk PbTe, which have their main axes along the

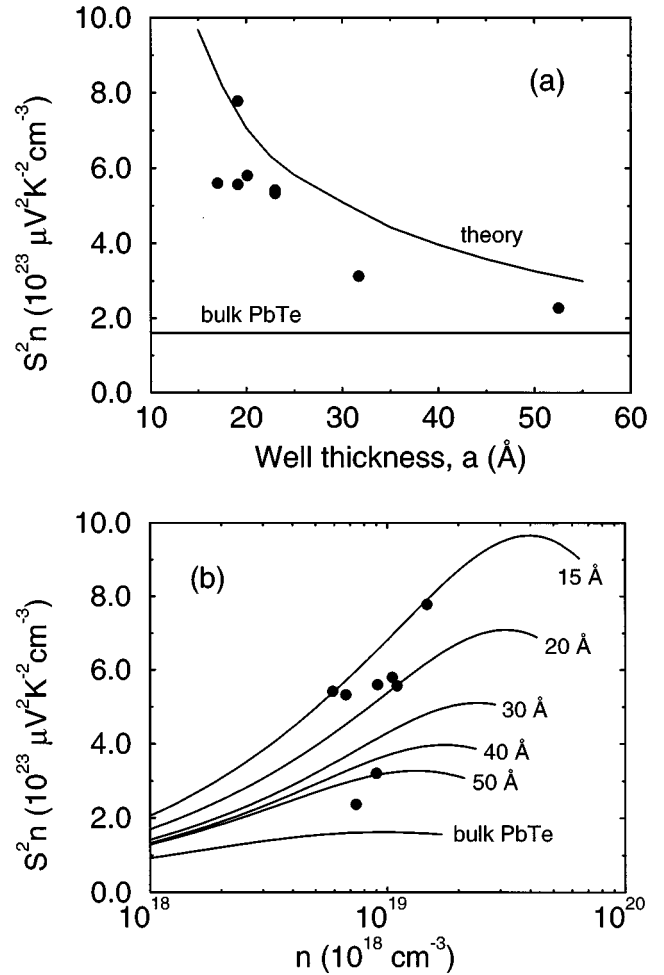


FIG. 1. (a) S^2n results for $\text{PbTe}/\text{Pb}_{0.927}\text{Eu}_{0.073}\text{Te}$ MQW's (full circles) as a function of well thickness a at 300 K. For comparison, the best experimental bulk PbTe value is also shown. Calculated results for optimum doping using our model are shown as a solid line. (b) S^2n results for the same $\text{PbTe}/\text{Pb}_{0.927}\text{Eu}_{0.073}\text{Te}$ MQW samples (full circles) as a function of carrier density n at 300 K. Calculated results using our model for different indicated well thicknesses are shown as solid curves.

$\langle 111 \rangle$ directions. Since growth occurs along the $[111]$ direction, one set of subbands is associated with the valley along the $[111]$ axis and has a circle as a surface of constant energy in the (k_x, k_y) plane. These are the longitudinal subbands. The other three valleys, with their main axis oriented obliquely to the $[111]$ growth direction, yield three ellipses as surfaces of constant energy in the two-dimensional case.⁷ Even though the Fermi level may lie just above the lowest-energy conduction-band subband, which is a longitudinal one, the oblique subbands may still contribute significantly to S^2n even though they are further from the Fermi level since they have a much higher density of states. Thus, to do a realistic calculation of the transport properties of PbTe quantum wells, it is necessary to know the relative energies of all four subband extrema and then to include all subbands in calculating the overall S and n .

The envelope function approximation (EFA) was used to calculate the positions of the energy levels in the MQW structures.⁷ The EFA calculation involves solving for the electron eigenstates in both the well and barrier materials,

and matching the wave functions at the interface with appropriate boundary conditions to find the energy levels and dispersion relations in the quantum well. Yuan *et al.*⁷ applied the EFA method to the PbTe/Pb_{1-x}Eu_xTe MQW system with great success and used it to reproduce their experimental optical data, without any fitting parameters. We used the same approach,⁷ to calculate the positions of the energy levels in our MQW samples. To use the EFA method, the band gaps, band offsets, interband momentum matrix elements, and far band parameters must be known. The band gap of PbTe is 319 meV at 300 K.⁸ We determined the band gap for our Pb_{0.927}Eu_{0.073}Te barrier material to be 630 meV from infrared transmission measurements of single layer samples. The band offsets were estimated by assuming the relation determined experimentally by Yuan *et al.*:⁷ $\Delta E_c/\Delta E_g = 0.55$, where ΔE_c is the conduction-band offset and ΔE_g is the difference in band gap between the well and barrier materials. Finally, the momentum matrix elements and far band parameters were obtained from Table III of Ref. 7. The positions of the quantum-well energy levels in the conduction and valence bands were thus obtained for several of our samples, and the results for a sample with a 53-Å well and a sample with a 20-Å well are shown as insets in Figs. 2(a) and 2(b), respectively. As a quick experimental check of our calculations, we did infrared transmission measurements on the same samples and the results are shown in Fig. 2. Yuan *et al.*⁷ showed that, for the PbTe/Pb_{1-x}Eu_xTe MQW system, there is a significant decrease in transmission when the incident photon energy equals the energy for the interband transition from the highest oblique subband in the valence band to the lowest oblique subband in the conduction band, the (1-1)^o transition. For the two samples shown in Fig. 2, the first oblique subband is the second subband in both the conduction and valence bands. Figure 2 shows that, for both samples, there is a steplike decrease in transmission at an energy almost exactly at that calculated for the (1-1)^o transition (see inset). The transition occurs at about 470 meV for the 53-Å well sample and at about 580 meV for the 20-Å well sample. For both samples, the transmission goes to zero at about 630 meV, which corresponds to the band gap of the barrier. It is very difficult to observe the (1-1)^l transition between the first longitudinal subbands in the valence and conduction bands because the longitudinal subbands have a very low density of states, much lower than that for the oblique subbands.⁷ The very good agreement between the infrared transmission results and our EFA calculations confirm that EFA calculations can be used to determine the positions of the subband energy levels in our samples. Our calculations also show very little dispersion in the direction normal to the layers, which is expected for 2D transport.

Once we had calculated the positions of the energy levels in the quantum wells, the next step was to calculate values for the Seebeck coefficient and carrier density within the framework of our theoretical model, using expressions for the Seebeck coefficient S_i and carrier density n_i of the i th subband² given by

$$n_i = \frac{1}{2\pi a} \left(\frac{2k_B T}{\hbar^2} \right) (m_1 m_2)^{1/2} F_0(\zeta_i^*) \quad (2)$$

and

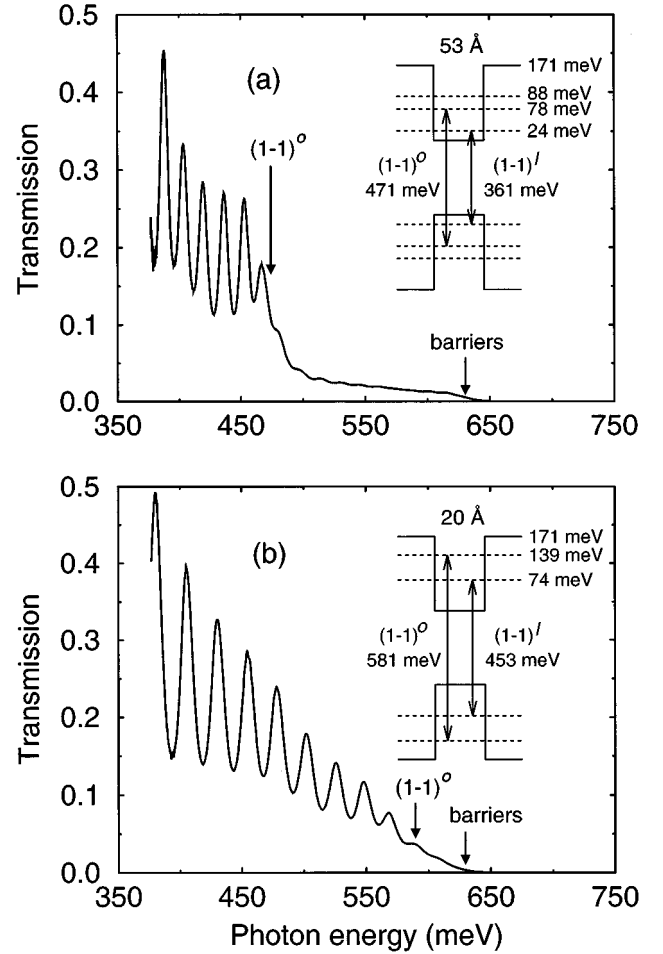


FIG. 2. Transmission vs photon energy at 300 K for (a) a MQW sample with a 53-Å well and a 560-Å barrier and (b) a MQW sample with a 20-Å well and a 430-Å barrier. Insets show the results of EFA calculations of the quantum-well energy levels and the interband transition energies.

$$S_i = -\frac{k_B}{e} \left(\frac{2F_1(\zeta_i^*)}{F_0(\zeta_i^*)} - \zeta_i^* \right), \quad (3)$$

where the function F_j for a Fermi-Dirac distribution is given by

$$F_j(\zeta_i^*) = \int_0^\infty \frac{x^j dx}{e^{(x-\zeta_i^*)} + 1}, \quad (4)$$

a is the width of the quantum well, m_1 and m_2 are the principal effective-mass components parallel to the layers, and $\zeta_i^* = (\zeta - E_i)/k_B T$ is the reduced Fermi level measured relative to E_i (the minimum energy of each subband calculated using the EFA method), where ζ is the Fermi level. For multiple subbands, the total carrier density and Seebeck coefficient are $n = \sum_i n_i$ and $S = (\sum_i S_i n_i) / (\sum_i n_i)$, assuming all subbands to have the same mobility as a first approximation and for lack of better experimental knowledge.

For our S and n calculations, we used a constant barrier thickness of 460 Å, which is the average thickness of all our samples shown in Fig. 1. We did calculations for different well thicknesses varying from 15 to 50 Å. The effective masses were extracted from the two-band momentum matrix

elements in Table III of Ref. 7. This gave a bulk longitudinal effective mass $m_{\parallel}=0.620m_0$ and a bulk transverse effective mass $m_{\perp}=0.053m_0$. For the 2D quantum well, this gives $m_1=m_2=m_{\perp}$ for the longitudinal subbands, and $m_1=m_{\perp}$, $m_2=0.283m_0$ for the oblique subbands. For each well thickness, we used the EFA calculation to get the positions of the energy levels, E_i . S and n were then calculated as a function of Fermi level ζ , and thus S and S^2n were found as a function of n . The calculated results of S^2n vs n for different well widths are shown as solid lines in Fig. 1(b). The calculated maximum S^2n for each well width [the peak of each curve in Fig. 1(b)] is shown vs well width as a solid line in Fig. 1(a), while Fig. 1(b) shows that the optimum doping increases as the quantum well width is decreased. As can be seen from Figs. 1(a) and 1(b), there is very good agreement between experiment and theory, especially considering that *no* adjustable parameters were used in our calculation. Therefore our experimental results appear to confirm the predictions of our theoretical model, showing that MQW structures may indeed be used to obtain a high Z .

So far, we have considered only S and n since it is through these properties that our theory predicts an increase in Z . However, Z depends also on the thermal conductivity κ . If we assume that the quantum well κ is the same as the bulk κ value, our experimental results in Fig. 1 imply that the quantum well Z may be up to five times greater than the bulk value, giving a value of $ZT=2.0$ at 300 K, twice the value of the best bulk thermoelectric materials. However, this value is for the quantum well alone, and even though all of the electronic transport is in the quantum well, the barrier layers do contribute to the total lattice thermal conductivity.

Due to the thick barriers, this will make the overall Z of the MQW structures about a factor of 20 less than the well values alone if we assume that the $\text{Pb}_{0.927}\text{Eu}_{0.073}\text{Te}$ has the same κ as bulk PbTe. It is likely, however, that due to alloy scattering, the barrier κ is significantly less than the bulk value, in which case the overall Z may be close to a useful value, even with thick barriers. Work is underway to measure κ of our MQW samples to determine the overall Z . In general, it is difficult to measure κ for thermoelectric thin films since κ is very low, leading to significant errors due to heat loss. Also, κ of the substrate is often much greater than that of the film, leading to another source of difficulty. Although we have needed wide barriers to ensure 2D well transport, it may be possible to increase the barrier Eu content to give a higher band gap so that thinner barriers can be used to confine the electrons in the wells.

In conclusion, we have done an experimental investigation to test our theoretical model which predicts an increase in Z in MQW structures. Good agreement was found between the experimental results and our calculations, giving apparent experimental confirmation of our model. This suggests that MQW structures may indeed attain an enhanced thermoelectric figure of merit.

The authors would like to thank G. Springholz, G. Bauer, and G. Dresselhaus for valuable discussions. We gratefully acknowledge support for this work by the U.S. Navy under Contract No. N00167-92-K0052. The Lincoln Laboratory portion of this work was sponsored by the Department of the Army, the Department of the Navy, and the National Aeronautics and Space Administration.

¹H. J. Goldsmid, *Thermoelectric Refrigeration* (Plenum Press, New York, 1964).

²L. D. Hicks and M. S. Dresselhaus, *Phys. Rev. B* **47**, 12 727 (1993).

³L. D. Hicks, T. C. Harman, and M. S. Dresselhaus, *Appl. Phys. Lett.* **63**, 3230 (1993).

⁴D. L. Broido and T. L. Reinecke, *Phys. Rev. B* **51**, 13 797 (1995).

⁵D. L. Broido and T. L. Reinecke, *Appl. Phys. Lett.* **67**, 1170 (1995).

⁶J. O. Sofo and G. D. Mahan, *Appl. Phys. Lett.* **65**, 2690 (1994).

⁷Shu Yuan, G. Springholz, G. Bauer, and M. Kriechbaum, *Phys. Rev. B* **49**, 5476 (1994).

⁸Shu Yuan, H. Krenn, G. Springholz, and G. Bauer, *Phys. Rev. B* **47**, 7213 (1993).

⁹G. Springholz, G. Ihninger, G. Bauer, M. M. Olver, J. Z. Pastalan, S. Romaine, and B. B. Goldberg, *Appl. Phys. Lett.* **63**, 2908 (1993).

¹⁰T. C. Harman, D. L. Spears, and M. J. Manfra (unpublished).